CAPE SIMULATIONS
Engineering Solutions Through Computer Simulation

TR/111176

COMPUTATIONAL SIMULATION OF CONTAINMENT INFLUENCE ON DEFECT GENERATION DURING GROWTH OF GeSi

[redacted]

Contract Number NAS8-98252
Final Report

Dec 24, 2001

Principal Investigator Shariar Motakef, Ph.D.

[redacted]

Reduction of Defects in Germanium Silicon

I. Summary

This report covers the work conducted in conjunction with the NASA activity denoted as the RDGS program. The RDGS activity is focused on identifying the impact of crucible containment on defect formation in Ge and GeSi crystals. To understand the effect of containment, a major part of the research effort has been focused on achieving detached growth in a Bridgman configuration. This report is not an exhaustive compilation of all the work done on RDGS at Cape Simulations. Rather, it consists of our major findings in the area of detached growth.

Detached growth can be considered at several levels:

1. Formation of detached growth
2. Stability of detached growth based on static force balance
3. Stability of detached growth to perturbations
4. Dynamics of detached growth: motion of the melt-gas-crucible line in tandem with the advancing solidification front, and factors controlling the crystal diameter so that it does not grow out to meet the containment.

This report primarily focuses on issues 2 and 3. Issues listed under 4 above are, however, fundamentally very important and least understood. In general stability of crystals grown from a meniscus, such as that shaped crystal growth championed by the Tatarchenkov, can not be used to answer the above questions for detached growth in Bridgman configuration. We remain confident that most answers to questions on detached growth will come from the issues listed under 4 above.

II. Pressure variation requirements across the liquid column: RDGS experiments in NASA

5. Section Summary

In this section we report on two parallel studies of the RDGS experiments. In the first study we focus on the fundamental issues, and in the second we use experimental conditions to simulate the growth process. In the former, we seek to identify the necessary conditions to achieve detached growth and in the latter, whether these conditions are achieved in the proposed experiments.

6. Fundamental Considerations

The fundamental approach in these experiments is straightforward. The ampoule is designed so that (a) a small volume of gas is trapped in the annular cavity separating the seed from a quartz liner, and (b) a larger gas volume is present above the melt free surface. In principle, the pressure difference between the two gas volumes can be exploited to maintain a layer of gas between the growing crystal and the quartz housing around it, and thus detached growth is maintained.

2.1 Hypothesis

The analysis and conclusions presented in this report are based on the hypothesis that:

- Detached growth is maintained, if the pressure in the gas trapped around the crystal is approximately equal to the sum of the pressure in the top reservoir, hydrostatic head of the liquid column, and the pressure drop across the melt-gas meniscus;
- If pressure in the trapped gas is higher than this value, bubbles will be formed leaving the annular volume around the crystal;
- If the pressure in the trapped gas is less than this value, the trapped gas column will collapse and the molten material will rush in to replace the trapped gas;

Statements 2 and 3 are expected to occur when the trapped-gas pressure deviates from the equilibrium value(statement 1) by some threshold values. Currently, we do not know what these threshold values are. Furthermore, we do not know to what extent (if any) reduced gravity increases the magnitude of these allowable deviations in the trapped-gas pressure. It should be noted that for "small" pressure deviations the diameter of the detached crystal will change with time. Our free surface analysis (see Figure 7) indicates that for a given melt/crucible contact angle, the diameter will change for fairly small deviations in the pressure of trapped gas. This, however, may be a much slower process than bubble generation or loss of trapped gas.

2.2 Calculation of Required Pressure in the Top Reservoir

Consider two situations as schematically shown in Figure 1. First, after melt back and prior to the start of growth process. Second, sometime during detached growth.

The lower-bound approximation to the pressure of the gas trapped after melt-back can be written as:

$$P_1^g = \frac{mRT_1}{V_1} = \frac{mRT_1}{AgL_1}$$

In the above Ag is the gap area which is equal to $2\pi r_c\delta$, where δ is the gap thickness and r_c crystal radius. As the crystal grows (referred to stage 2) and the gap length goes from L_1 to L_2, pressure P_2^g becomes (for constant temperature of trapped gas)

$$P_2^g = P_1^g \frac{L_1}{L_2}$$

Denoting the pressure in the top reservoir at P^T, one can write the following equilibrium equations:

$$P_1^T = P_1^g - \rho g h_1 - \Delta P_\sigma$$

$$P_2^T = P_2^g - \rho g h_2 - \Delta P_\sigma$$

In the above the second term on the right hand side denotes the hydrostatic head of the liquid column, and the third term the pressure drop due to surface tension at the meniscus. One can rewrite the last equation to obtain a relationship between the required top pressure with increasing crystal length ΔL

$$P_2^T = P_1^g \frac{L_1}{L_1 + \Delta L} - \rho g(h_1 - \Delta L) - \Delta P_\sigma$$

Another equally useful equation can be obtained for the *required* change in the top pressure with growth:

$$P_2^T - P_1^T = P_1^g \left[\frac{L_1}{L_1 + \Delta L} - 1 \right] + \rho g(\Delta L)$$

To better appreciate the implications of the above equations, they are evaluated at conditions corresponding to the proposed experiments and listed in Table 1. The Table entries are based on the conditions at melt-back (i.e. initial conditions) which are obtained from the detailed modeling results described in the next section. Simulation results indicate that the pressure in the trapped gas at melt back would be 2.354×10^5 N/m^2 and the height of trapped gas (i.e. seed length after melt-back) L_1 = 2.54 cm. The

required pressure in the top gas reservoir at melt back is 2.272×10^5 N/m^2. The term T_2^T in the table denotes the *required* mean temperature of the gas in the top reservoir.

Table 1. Pressure and temperature calculations at conditions considered to lead to detached growth in the RDGS experiments.

ΔL (cm)	$P_1^g\left[\frac{L_1}{L_1+\Delta L}-1\right]$ N/m^2	$\rho g(\Delta L)$ N/m^2	$P_2^T - P_1^T$ N/m^2	P_2^T N/m^2	$\frac{P_2^T}{P_2^T(\Delta L=0)}$	T_2^T (K)
0	0	0	0	2.27×10^5	100.0%	1135
0.5	-3.93×10^4	2.45×10^3	-3.69×10^4	1.90×10^5	83.7%	951
1.0	-6.74×10^4	4.90×10^3	-6.25×10^4	1.65×10^5	72.7%	823
2.0	-1.05×10^5	9.80×10^3	-9.52×10^4	1.32×10^5	58.2%	660
3.0	-1.29×10^5	1.47×10^4	-1.14×10^5	1.13×10^5	49.8%	566
4.0	-1.45×10^5	1.96×10^4	-1.25×10^5	1.02×10^5	44.9%	508
5.0	-1.57×10^5	2.45×10^4	-1.32×10^5	0.95×10^5	41.8%	475

2.2.1 Features of Data in the Table

- The hydorstatic head (col 3) is small relative to the pressure of the trapped gas and the gas reservoir.
- After growth of a 5 cm sample, the pressure in the top reservoir (col 5) must be reduced appreciably by close to 1 atm. Thus, the new pressure in 42% of the original pressure in the top reservoir (col 6).
- The required reduction of pressure in the top reservoir with growth implies a reduction of the reservoir's mixed-mean temperature. Using perfect gas law and an initial temperature of 1135 K, this implies that the top reservoir temperature has to be reduced to 475 K (col 8) during a 5 cm crystal growth exercise.

7. Discussion

The above calculations imply the following chain of causality.

1. The initial pressure in the ampoule at room temperature determines the pressure of the trapped gas at melt-back (P_1^g), assuming that the trapped gas occupies the same volume at room temperature as it does at melt back.

2. The required pressure in the top reservoir, P_1^T, is equal to the sum of the liquid hydrostatic head, the pressure drop across the meniscus, and P_1^g.
3. The required pressure in the top reservoir establishes the required average temperature in the gas reservoir (through perfect gas law).
4. The required reservoir's mean temperature and the prevailing temperature gradient along the reservoir establish (approximately) the required length of the top gas reservoir.
5. Assuming one has the required pressure in the top reservoir, then with growth this pressure has to be lowered to accommodate the decreasing pressure of the trapped gas as it expands with increasing crystal length. For example, once the length of the grown crystal equals the length of the seed at melt-back, the volume of trapped gas has increased by a factor of two. Making a conservative approximation that the mean temperature of the trapped gas has not changed from the value at the beginning of growth, the pressure in the trapped gas would be reduced by half. This translates, in essence, to a reduction by a factor of two in the required pressure in the top reservoir, and an associated reduction (by a factor of 2) of the mean reservoir temperature. This is a major reduction which in all likelihood will interfere with growth.
6. As a first approximation there is a direct relationship between the ratio of crystal/seed length and the reqiured reduction of pressure and temperature in the top reservoir. That is, for a crystal/seed length ratio of 2, the reservoir temperature and pressure have to be reduced by a factor of 2. This required reduction can be lowered if one considers the reduction of the temperature (thus pressure) of the trapped gas with growth; however this would not be significant. For example, with a (large) temperature gradient of 100 C/cm on the crystal side and a seed length of 2.5 cm, the average temp of the trapped gas would be 1085 K. With 2.5 cm of crystal grown, it falls to 960 K. If one accounts for this change of temperature, the trapped gas pressure after 2.5 cm of growth is 44% of the initial pressure. If one ignores this change of temperature, it would be 50%. As indicated above, this is a small correction.

8. Implications

The fundamental calculations in this section indicate that for a fixed mass of trapped gas, the gas reservoir pressure and temperature have to be reduced appreciably during growth, **IF** the length of grown crystal is appreciable relative to the length of the seed at melt back. Practical considerations suggest that the seed at melt-back must be long enough so that the length of grown crystal would increase the volume of trapped gas by no more than 20-30%, requiring a 20-30% reduction in the temperature and pressure of the top reservoir.

9. Detailed Numerical Simulations

5.1 Preliminaries

A finite element thermal model of the planned growth ampoule, Figure 2, was developed. The temperature profile of the furnace liner was modeled to be determined by the setpoints provided by the MSFC group for three stages of growth as shown in the following table. The furnace liner temperature is assumed to vary linearly between the set points[1]. The temperature profile along the outer periphery of the quartz and the corresponding set points for stage 1 is shown in Figure 3.

Table 2. RDGS Experimental Set points

Position of T/C From Bottom of Zone 6 in mm	Temperature at Stage 1 (8 hrs) K	Temperature at Stage 2 (10 hrs) K	Temperature at Stage 3 (12 hrs) K
165	1233.18	1109.88	1067.65
91	1277.32	1260.01	1212.50
60	1223.03	1212.01	1183.12
29	1202.8	1194.31	1161.08
19	1141.55	1128.08	1092.94
5	946.43	927.29	892.23

The gap size between the crystal and the quartz insert (Figure 1) is equal to .05 mm at room temperature. At melting point temperature of Ge, the differential expansion of quartz and Ge[2] results in a smaller gap thickness of .038 mm.

The pressure drop across the meniscus separating the liquid and the trapped gas is based on the solution of Laplace-Young equation with the following parameter values: growth angle 10°, wetting angle 115° , surface tension 0.4 N/m.

5.2 Simulation Results

5.2.1 Stage 1, After 8 Hours

The temperature field in the charge at this stage is shown in Figure 4. Results indicate:

- The position of growth interface is 2.49 cm above the bottom of the seed. We refer to this as the melt-back position.
- Average temperature of Ar above the melt is 1250 K. This translates to a pressure of p_{Ar}=2.5 bar.
- Average temperature of trapped Ar in the gap is 1177K.
- Pressure of Ar in the gap is calculated to be 2.354×10^5 N/m^2. This calculation is

[1] The temperature measurements reported on an ampoule containing Si are inconsistent with the furnace setpoints reported for the same experiment. That is, the temperatures measured on the ampoule are higher than the set points. Accordingly, we chose to use the furnace set points, until this discrepancy is resolved.

[2] Linear thermal expansion coefficient for Ge and quartz are 5.7×10^{-6} K^{-1} and 5.7×10^{-7} K^{-1}, respectively.

back and equal to the initial density of Ar at room temperature. That is, the ratio of pressure to temperature remained constant[3].

- The calculated pressure in the top reservoir is higher than the pressure in the gap, whereas fundamental considerations indicate that it should be smaller. It is larger than the required pressure value of 2.27 x10^5 N/m^2. Thus, there is a pressure imabalance.
- Alternatively, the reservoir's temperature of 1250 is higher than the required value of 1135 K.

We do not have the tools to establish whether the excess pressure of about 0.23 atm in the top cavity is sufficiently large to force the melt into the gap around the seed.

5.2.2 Stage 2, After 10 Hours

The temperature field in the ampoule is shown in Figure 5. Results indicate that:

- Position of the interface is 3.38 cm above the bottom of the seed
- Average temperature of Ar above the melt is 1169 K, implying an Ar pressure of 2.338 x 10^5 N/m^2
- Average temperature of trapped Ar between the crystal and the inner crucible is 1171 K.
- With the average temperature of the trapped Ar essentially the same as in the previous case, its pressure is calculated to be 1.734 x 10^5 N/m^2.
- The calculated pressure in the Ar reservoir is about .6 atm higher than the required value of 1.734 x 10^5 N/m^2.
- The required reservoir temperature is 586 K (!), which is lower than the calculated value by 583 K (!)

5.2.3 Stage 3, After 12 Hours

The temperature profile for this stage indicates that the entire melt is frozen, Figure 6.

10. Sensitivity Analysis

The calculated values of meniscus pressure-drop are influenced by the assumed values of growth angle α_o and contact angle θ. Figure 7 shows the variation of this value over a range of the two angles (α_o varying from 7 to 12° and θ varying between 70° and 120°). Results indicate a weak sensitivity to α_o and a stronger variation to θ. As the calculated reservoir pressure for both stages is higher than those of the trapped Ar, the variations of meniscus pressure with α_o and θ can not correct for this deviation. In sum, possible errors associated with the assumed values of α_o and θ are not large enough to bring the calculated values of reservoir pressure close to the required values. Overall, the

[3] An alternative scenario may correspond to the situation where the melting process would start from the top of the solid and all the gas contained between the charge and quartz is compressed down towards the seed as the melting front proceeds. This would yield a higher pressure for the trapped Ar.

meniscus pressure drop does not play an important role in the present calculations, and thus possible errors due to assumed values of contact and growth angles are unimportant.

The calculated pressures are much more strongly impacted by the assumed furnace temperature profile. The furnace temperature profile directly influences the three primary parameters. First, the pressure in the top reservoir. Second, the length of the seed at melt-back, thus the initial volume of the trapped gas. Third, the temperature of the trapped Ar, and thus its pressure during growth.

11. Conclusions

Simulations and fundamental considerations indicate that, for the assumed furnace temperature profile, the reservoir pressure is higher than the required value by non negligible amounts. These deviations are sufficiently large not to be attributable to modeling errors or inaccuracy in thermo-physical properties. These results suggest that the furnace set points and the ampoule design be re-evaluated. The first step in this direction would be the selection of a furnace for detailed modeling and adoption of a profiling technique that would generate results that could be compared with the calculations. Once in this manner the range of possible temperature profiles is determined, attention can be focused on ampoule design. Alternatively, we can start with an ampoule design and identify furnace conditions that would yield the necessary pressure in the top reservoir. The draw back here is that one may end up with temperature profiles which cannot be obtained in any of the available furnaces.

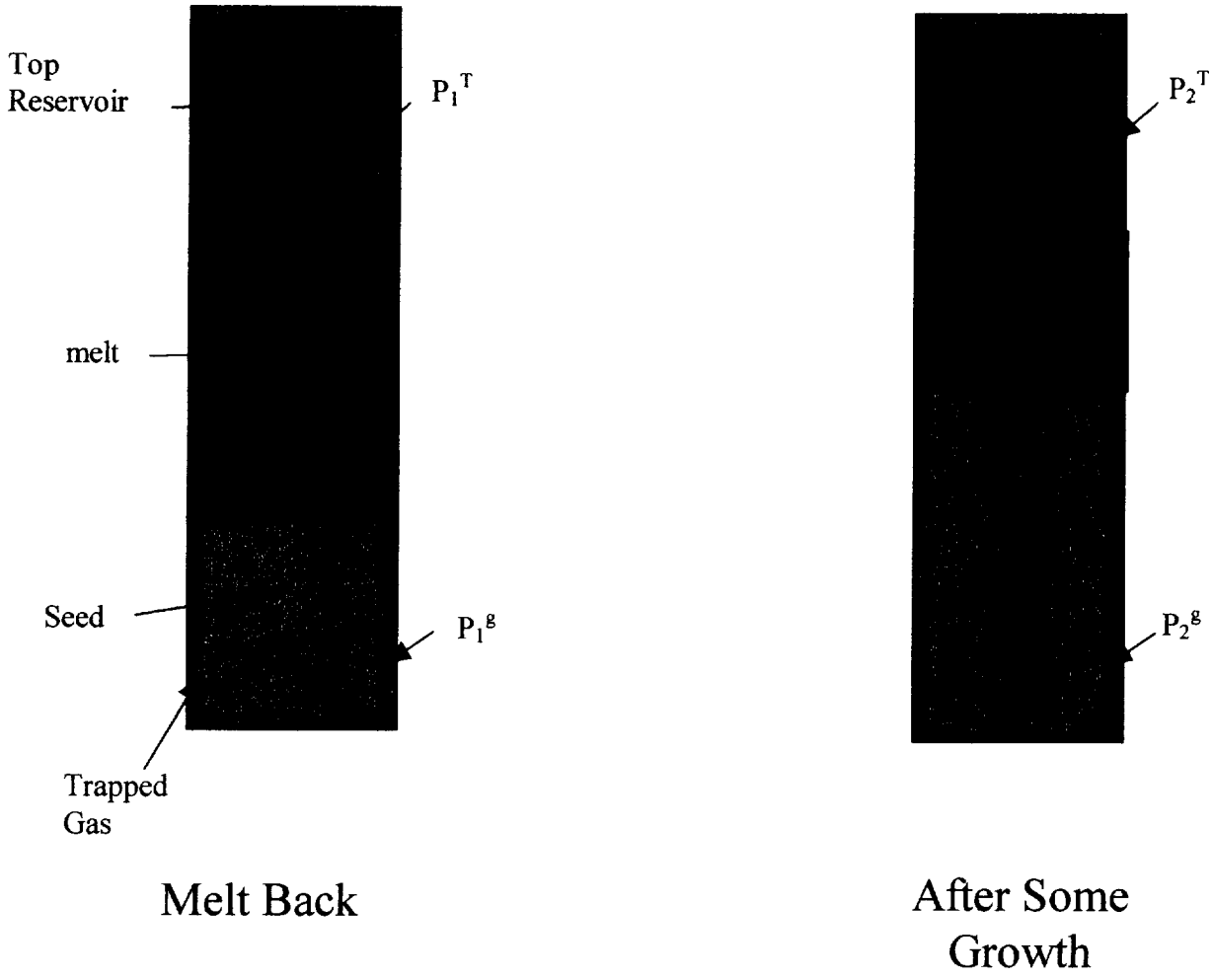

Figure 1. Schematic of the gas entrapment mechanism during meltdown.

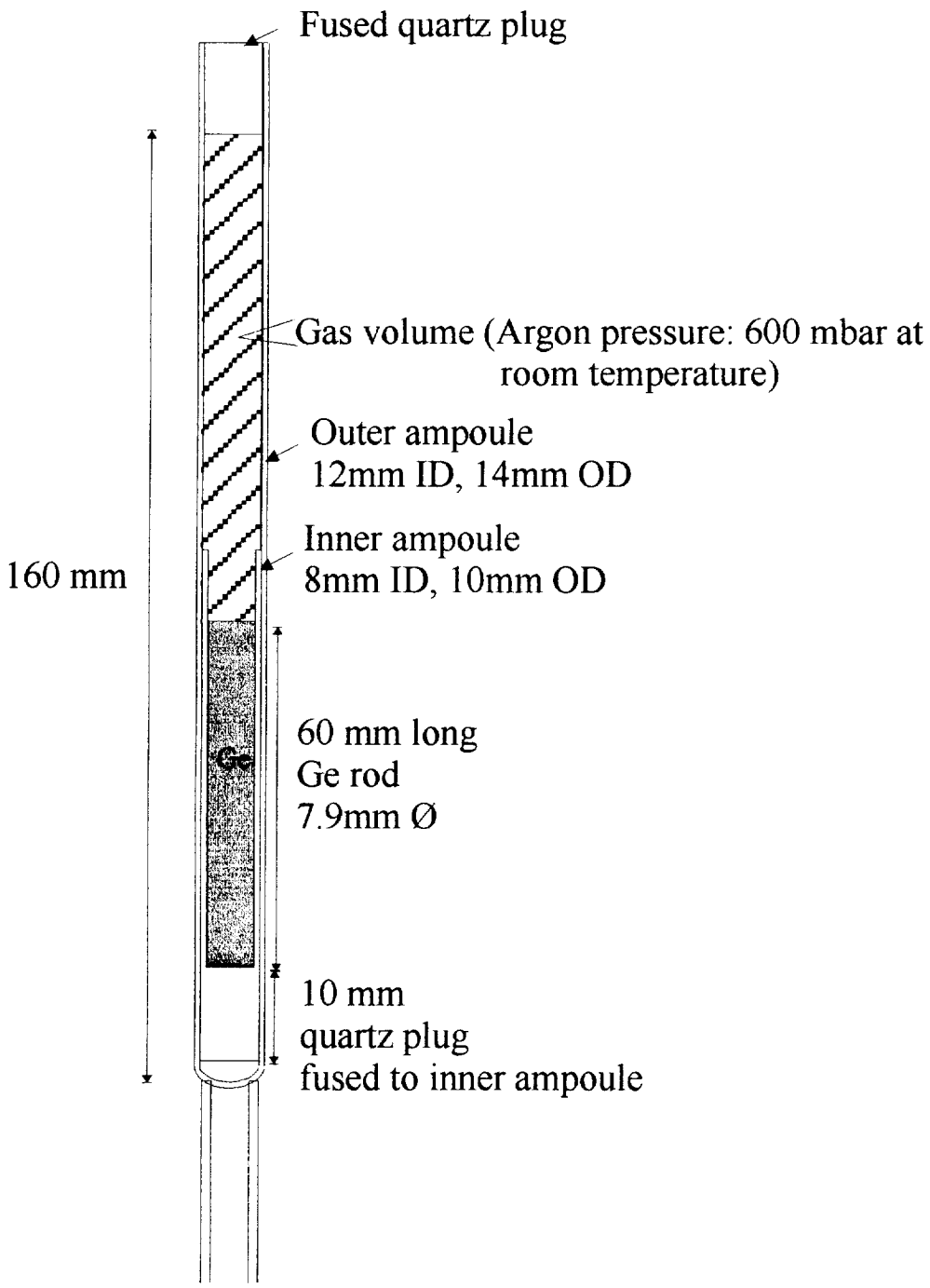

Figure 2. Schematic of the ampoule used in the first series of experiments.

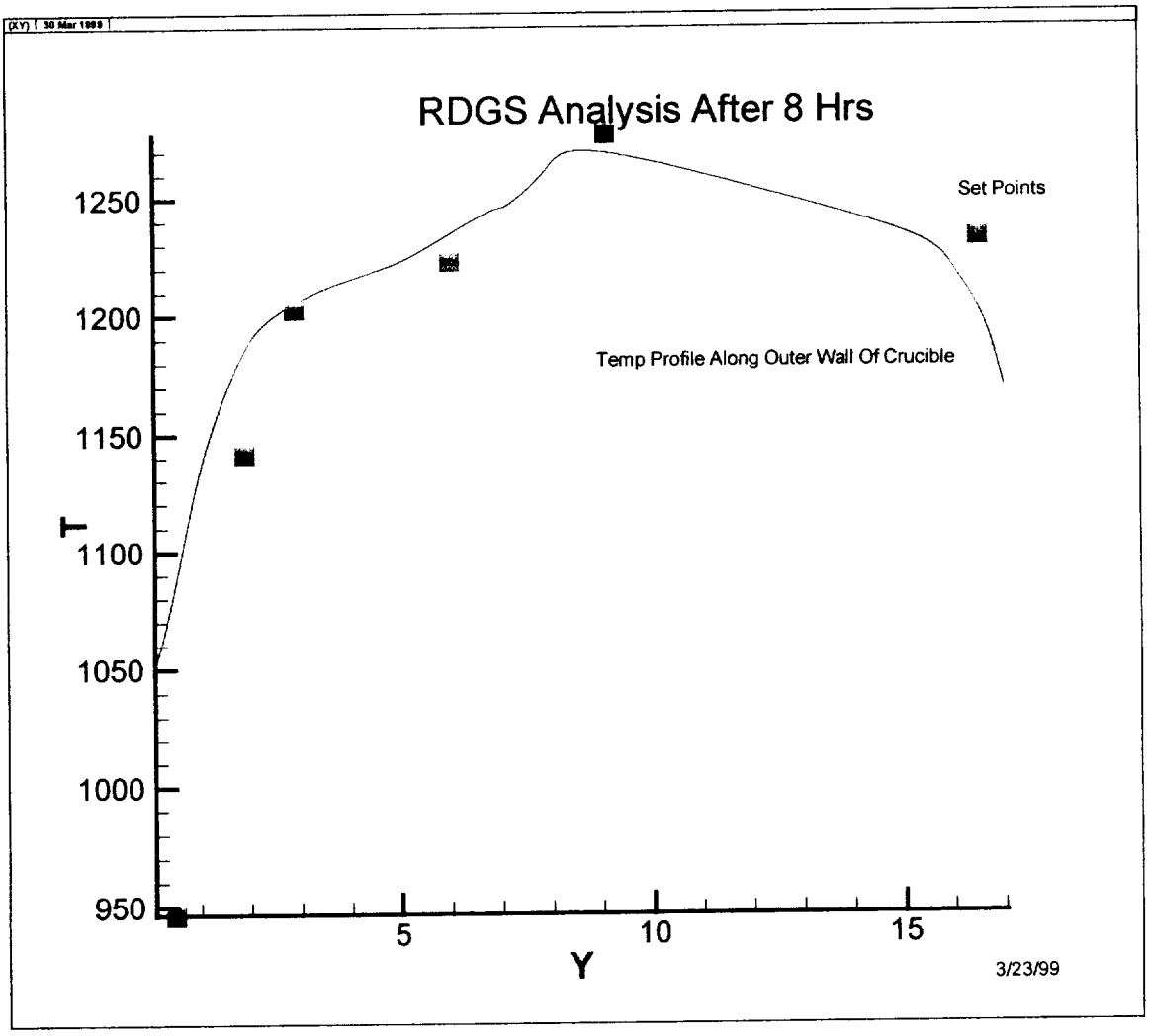

Figure 3. Temperature profile along the crucible

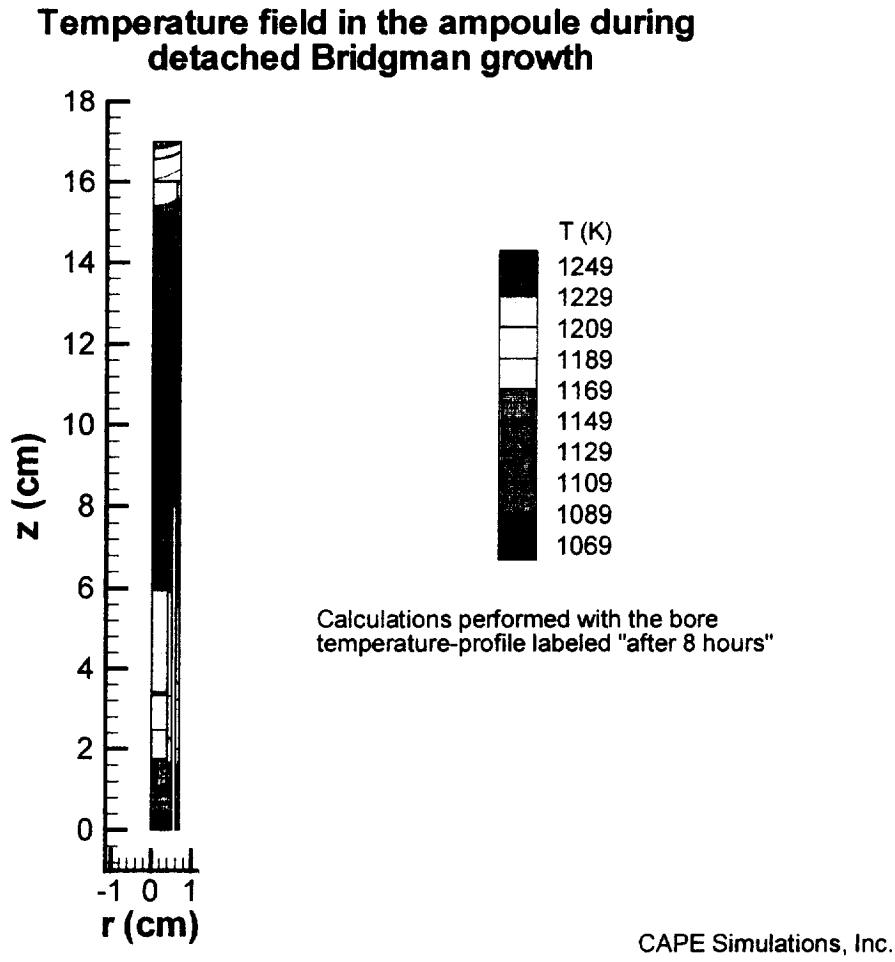

Figure 4. Calculated temperature profile in the cartridge, 8 hours into growth.

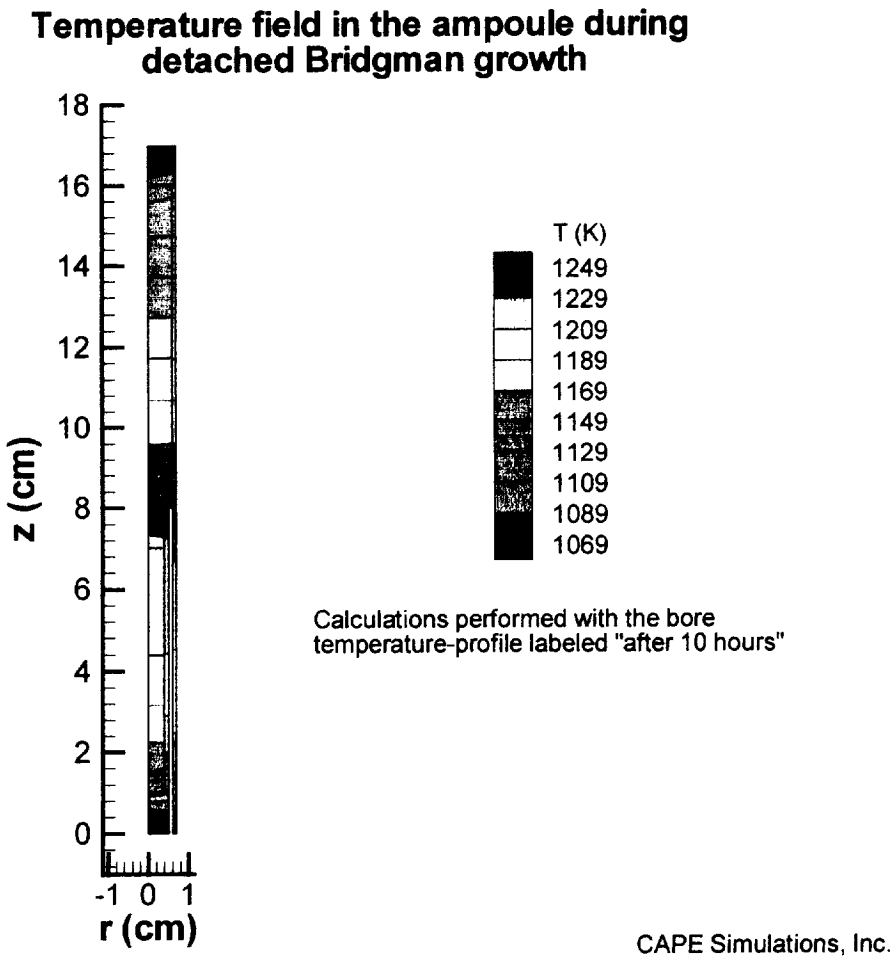

Figure 5. Calculated temperature profile in the ampoule, 10 hours into growth.

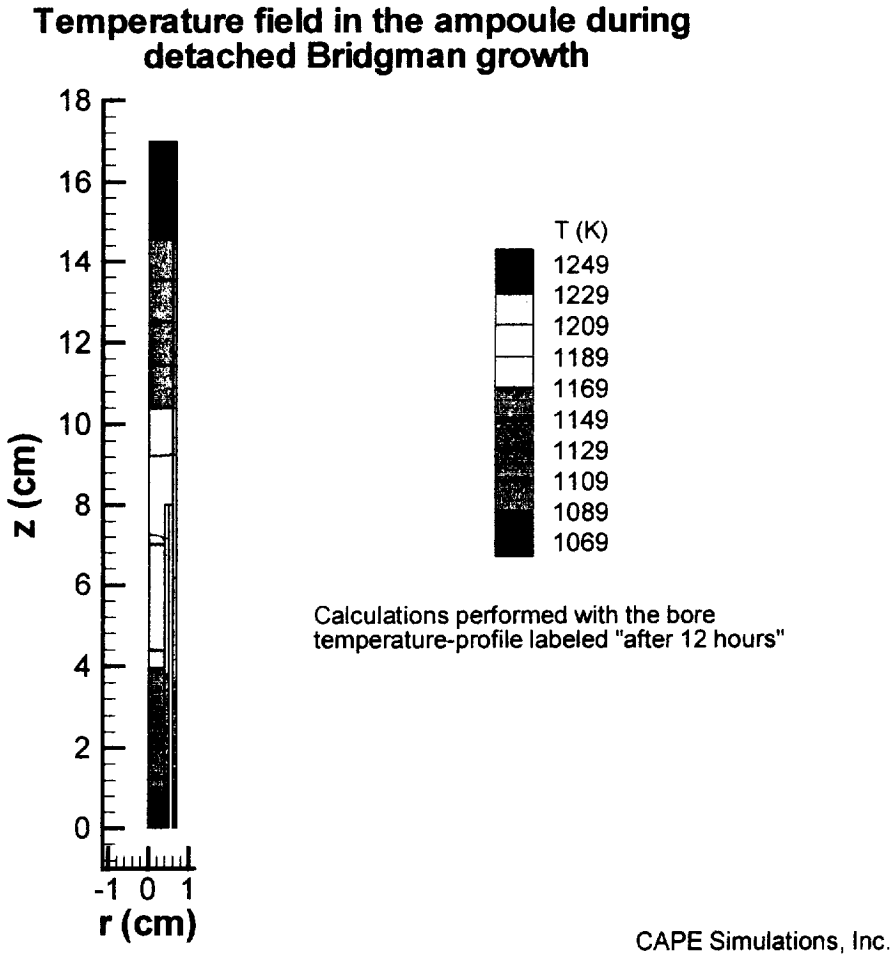

Figure 6. Calculated temperature profile in the ampoule, 12 hours into growth.

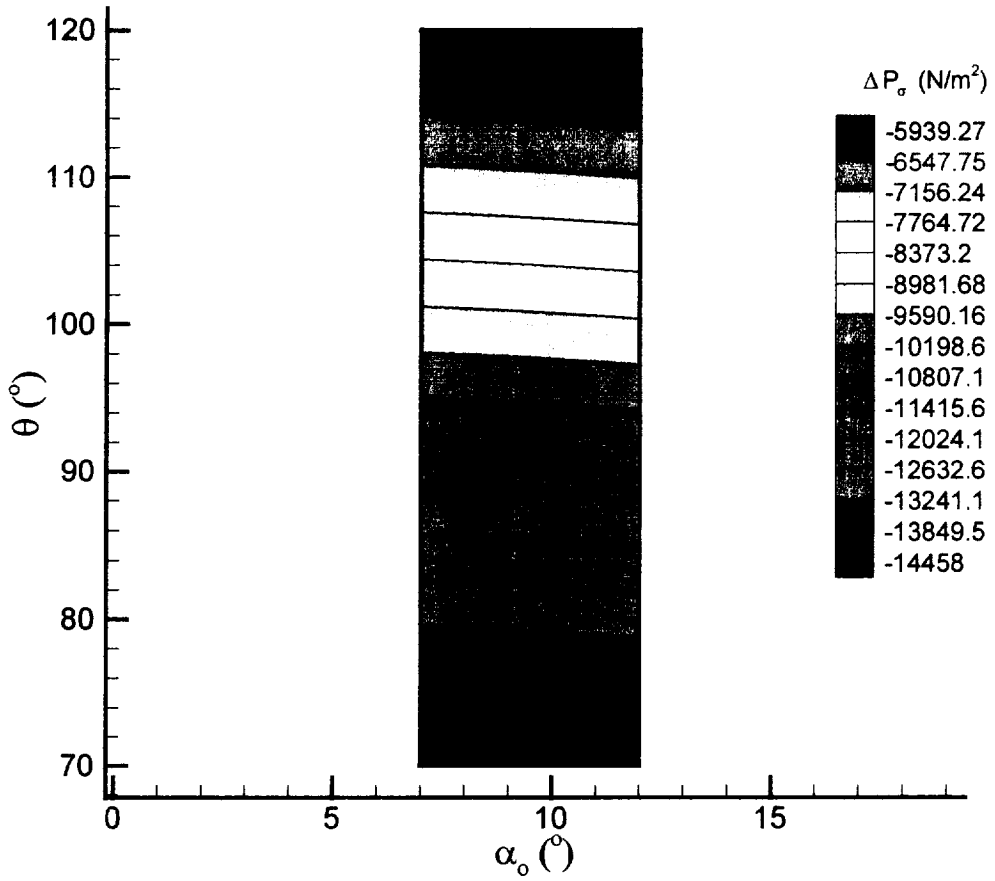

Figure 7. Calculated values of meniscus pressure-drop are influenced by the assumed values of growth angle α_o and contact angle θ.

III. Stability of detachment

1. Introduction

This section focuses on stability of the detachment gap after it has been formed. As the metric of stability we use the sensitivity of the gap thickness to perturbations in the parameters that control detachment: pressure of the gas in the detached gap, pressure of the gas at the upper free surface of the melt column, hydrostatic head of the liquid column, and the melt surface tension. We will show that the gap thickness and its sensitivity is a strong function of the contact angle between the melt and the crucible. We will further show that the gap thickness sensitivity is significantly reduced at low values of gravity, indicating a higher probability to achieve stable detached growth in space.

2. Analysis

The growth system under analysis is schematically shown in Figure 1. Detailed view of the meniscus is shown in Figure 2.

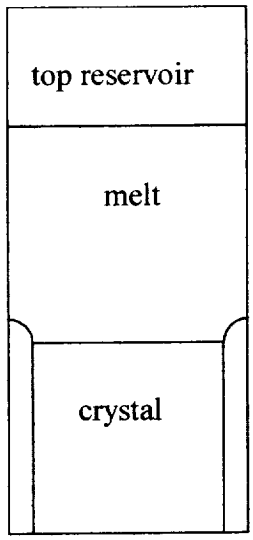

Figure 1. Schematic of the growth system.

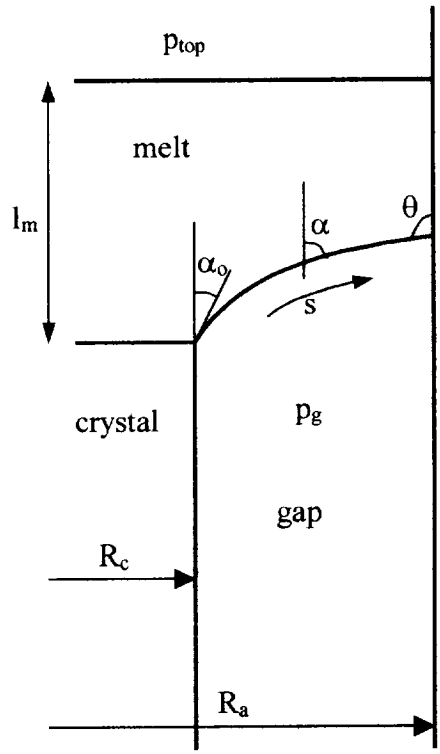

Figure 2. Schematic of meniscus identifying relevant geometrical and physical parameters.

The analysis reported here is based on the equations governing the static balance of forces in the meniscus around the growth interface during detached growth. These equations, generally referred to as Young-Laplace equations, are used to calculated shape of the detached meniscus at various values of the controlling parameters. These results are then used to calculate the stability metric described above. It is important to note that our stability metric does not in of itself indicate presence or absence of stability. Rather, it is a relative indicator which rank-orders the sensitivity of the gap to various conditions. Comparison of this information with existing experimental evidences will be used to infer conditions that will result in detached growth on Earth versus those for which space processing is required.

The Young-Laplace equations are shown below in non-dimensional form. In the above all length scales are non-dimensionalized by the ampoule radius R_a, R stands for radial direction, Z for axial direction measured from the location of the growth interface, S direction along the meniscus. The angle α is the angle that the meniscus makes with respect to the z axis and has the value of growth angle at the crystal-melt-gas tri-junction.

$$\frac{dR}{dS} = \sin\alpha$$

$$\frac{dZ}{dS} = \cos\alpha$$

$$\frac{d\alpha}{dS} = \frac{\cos\alpha}{R} + ZBo - \Pi$$

In this formulation the various controlling parameters are lumped into two non-dimensional numbers Bo and Π which capture the influence of material properties and pressure difference, respectively:

$$Bo = \frac{\rho g \ R_a^{\ 2}}{\sigma}$$

$$\Pi = (P_{Top} + \rho g h - P_{gap})\frac{R_a}{\sigma}$$

where P_{Top} is the pressure on the top surface of the liquid column, h is the height of melt column, and P_{gap} is the pressure below meniscus. The Bond number (Bo) captures the influence of gravity relative to the surface tension forces, and Π captures the relative influence of the pressure difference to the capillary forces. As gravity is reduced the Bond number decreases and becomes inconsequential in determining the shape of the meniscus. Thus, at sufficiently low values of gravity the shape of the meniscus is insensitive to the value of gravity and is determined solely by the parameters in Π, namely the pressure drop across meniscus, ampoule radius, and surface tension of the melt. Thus, the parameters included in Π uniquely determine the equilibrium crystal radius (or equivalently the detachment gap) in space.

In general, the Young-Laplace equations are solved along the following lines. For a given value of Bo and Π a certain crystal radius is assumed and the above three equations are integrated along the meniscus starting from the crystal-melt-gas tri-junction; the boundary condition at this point is that α be equal to (the material-dependent) growth angle. These equations are integrated until the meniscus contacts the ampoule. If the contact angle constraint is not satisfied at that point, then the calculation procedure is repeated with a new crystal radius. This procedure is repeated until the correct contact angle is obtained at the melt-ampoule-gas tri-junction.

The analysis reported below is done for GeSi properties, except when the influence of contact angle is explored.

3. An Experimental Observation

The results presented below must be considered with the background of one important experimental observation.

Experiments conducted as part of this work have shown that on Earth the gas pressure in the gap below the meniscus cannot significantly exceed the sum of hydrostatic head, the pressure at the melt free surface, and the pressure drop across the meniscus. Once this limit is exceeded the gas trapped below the meniscus generates bubbles which rise around the melt column. In terms of our analysis this observation translates to the constraint that the minimum value of Π on Earth is close to zero.

4. Results

4.1 Fundamental Behavior

A representative set of meniscus shapes on earth for a range of values of $P_{gap} - P_{Top}$ is shown in Figure 1. These results indicate several important issues:

- For larger values of $P_{gap} - P_{Top}$ the meniscus is convex and detachment gap is fairly small.
- As the pressure of the gas below meniscus is lowered relative to the pressure at the melt free surface, the crystal diameter decreases (detachment gap starts to widen) and then it reverses and starts to increase. In Figure 1 this phenomenon is observed around $P_{gap} - P_{Top}$ of 5059 N/m^2. Pressure differences lower than this value result in appearance of hour-glass shaped meniscus shapes. With further decreases in the in pressure difference the lower part of the meniscus starts approaching the crucible wall. At a pressure difference of 5010 the crystal re-attaches to the crucible.
- The range of pressure differences that would cover a very wide range of meniscus shapes is fairly small: roughly a 10% change in the pressure difference results in the collapse of the meniscus.
- The hydrostatic head for the case studied is about 5200. Thus, the above results indicate that it is possible to get detached growth at conditions where the gap pressure is lower than the hydrostatic head. The meniscus shape would have the hour-glass shape under these conditions. It should be noted that this is a small region of existence. A 5% change in the gap or top pressures would result in the collapse of the meniscus.

A similar set of data for 10^{-6} g is shown in Figure 2. These results indicate a substantially different behavior:

- The elimination of hydrostatic head implies that detachment can be achieved over a much wider range of pressure differences $P_{gap} - P_{Top}$.

- As the gap pressure falls below that of the top pressure, the system responds by monotonically decreasing the crystal radius.

4.2 Influence of Contact Angle on Gap Thickness

The influence of contact angle on thickness of detachment gap is explored in Figures 3 and 4 for 1g and 10^{-6} g, respectively.

- Both sets of calculations reveal that the gap thickness decreases with increasing difference between the pressure in the gap and melt top. In Figure 3 we have inserted a vertical dashed line to indicate that only values of pressure to the left of this line are realizable on earth. Higher values would result in bubbling. formation.

- A more interesting observation is that the gap thickness decreases appreciably with increasing contact angle. Thus, for otherwise identical values of P_{gap}-P_{top} , increasing the contact angle from 125 to 169 degrees decreases the gap thickness by more than one order of magnitude. The effect of gravity appears primarily at low values of P_{gap}-P_{top}, where the plotted curves turn downwards. Other than this effect the overall behavior, particularly the influence of contact angle, is similar.

4.3 Sensitivity of Gap Thickness

The sensitivity of gap thickness to the pressure difference across the melt is explored in the next two figures. Figures 5 and 6 show plots of non-dimensional derivative of gap thickness with respect to the non-dimensional pressure Π ($de/d\Pi$) versus the non-dimensional pressure. We consider this parameter to be a direct indicator of the "stability" of the detachment gap. The outstanding features of these results are:

- The gap sensitivity goes down with increasing gap pressure, or equivalently gap thickness.

- The gap sensitivity is strongly influenced by the contact angle. At otherwise identical conditions, the gap sensitivity parameter is lowered by close to two orders of magnitude when the contact angle is increased from 125 to 169 degrees.

- It must be noted, again, that as the dashed line in Figure 3.2-5 indicates at 1g the gap pressure can not exceed a certain value due to possibility of bubbling. In microgravity, however, we can arbitrarily increase the gap pressure to reduce the sensitivity of the gap thickness to perturbations in non-dimensional pressure Π.

- Another important issue regarding operation in microgravity is the stability of detached growth for a fixed volume of trapped gas. That is, if a fixed volume of gas is trapped below the meniscus, its pressure decreases as its volume increases with increasing crystal length, as well as the reduction in its average temperature. The present results indicate if a sufficiently large amount of gas is trapped below the meniscus yielding a large value of $P_{gap} - P_{Top}$, then as the gap pressure decreases with growth it will stay stable. This is in contrast to growth on earth where the gas below the gap cannot be pressurized.

4.4 Influence of Growth Angle

A growth angle of 9 degrees was used in this analysis. Variation of this parameter in the reasonable range of 7-12 degrees did not lead to any significant changes in the results obtained above.

4.5 Influence of Wetting Angle

where $R=r/R_a$, $Z=z/R_a$ (z coordinate is measured from the growth interface), $S=s/R_a$, $Bo(=\rho_m g R_a^2/\sigma)$ is Bond number, and $P_o=(p_{top}+l_m\rho_m g-p_g)R_a/\sigma$.

For the zero-g (i.e. no-gravity) case, the Laplace Young equations have the analytical solution given by:

$$\cos\alpha = \frac{\cos\theta - \Pi/2}{R} + \frac{\Pi}{2}\frac{r}{R_a}$$

which yields the following equation for non-dimensional crystal radius $R_o=R_c/R_a$:

$$\frac{\Pi}{2}R_o^2 - \cos\alpha_o R_o - \cos\theta - \frac{\Pi}{2} = 0$$

Denoting the nondimensional gap width as e $(=1-R_o)$, we obtain the following expression for the rate of change of the gap width with respect to the wetting angle (i.e. $\partial e/\partial\theta$) for the zero-g case:

$$\frac{\partial e}{\partial\theta} = \frac{\sin\theta}{\Pi(1-e) - \cos\alpha_o}$$

The equivalent of the above equation for the one-g case can be obtained numerically. We use $\partial e/\partial\theta$ as a sensitivity parameter of the gap width to the wetting angle. Figure 8 shows the variation of $\partial e/\partial\theta$ with respect to θ and Π. The one-g results map onto the zero-g results for large negative values of Π; the reason for this is explained later. The dramatic change in the behavior as Π becomes positive is indicative of a fundamental

change in the force balance. At this point the one-g results for this case were not obtainable due to numerical uncertainties.

For all curves in Figure the maximum gap width was 100 μm. Before we proceed any further, it should be noted that for range of negative Π shown in Figure the gap width decreases with increase in the wetting angle, whereas for Π =2 the opposite is true (i.e. the gap width decreases with decrease in the wetting angle).
Effect of gravity on the gap width is twofold:

- Due to potential bubbling on earth we are restricted to operating at pressures in the gap close to $p_{top}+l_m\rho_m g$. This restriction is removed if we operate in micro-gravity.
- Gravity influences the meniscus shape, and therefore the gap width, through term Z×Bo. Thus, one can see that effect of gravity can be neglected if $|Z\times B_o| << |\Pi|$. Our meniscus shape calculations have shown that for large negative Π (i.e. sum of the top pressure and the hydrostatic head smaller than gas pressure in the gap) the meniscus is arc shaped, and that the height of the meniscus is comparable to the gap width. Therefore, for large negative values of Π , $Z\times B_o$ is negligibly small. With further decrease of the pressure in the gap, as Π approaches and exceeds zero, the meniscus shape changes from an arc to an hourglass. This change in the meniscus shape results in increase of the meniscus height, which coupled with decrease in the magnitude of Π makes the term $Z\times B_o$ comparable in magnitude to Π. This effect is evident in Fig. 7 , for Π=-4 and Π=-2, as the divergence between the one-g and zero-g data.

From Figure 7 we can ascertain the following:

- Sensitivity of the gap width ($|\partial e/\partial\theta|$) to the wetting angle decreases with increase in the wetting angle for a constant Π.
- For the same wetting angle, systems that operate at higher Π (lower p_g) are more sensitive to the changes in the wetting angle than systems that operate at lower Π (higher p_g).

These conclusions can be used to explain propensity towards detached growth, on earth, in ampoules for which the wetting angle is large.

Results of this study suggest that systems operating at high pressures in the gap (lower Π) are less sensitive to changes in the wetting angle during growth than ones operating at lower pressures in the gap (higher Π). The possible causes of changes in the wetting angle during growth may include variations in: ampoule material composition, compositional change of the melt during growth of alloys, temperature effects on surface tension. Therefore, in micro-gravity we should operate at the largest negative Π that system allows to minimize sensitivity of the gap width to possible variations of the wetting angle. It should be noted that this analysis is based on an axi-symmetric model, and therefore assumes azimuthal uniformity of the contact angle. Therefore, it does not address possible stability issues caused by azimuthal variations in the contact angle.

4.6 Summary of Results

The results presented above can be summarized as:

1. Gap thickness decreases strongly with increasing contact angle.
2. Large values of $(P_{gap} - P_{Top} - \rho gh)$ can be only achieved in space; on earth bubbling will set in.
3. Gap thickness decreases with increasing values of $(P_{gap} - P_{Top} - \rho gh)$
4. The detachment sensitivity parameter de/dΠ decreases strongly with increasing contact angle
5. de/dΠ is small for large values of $(P_{gap} - P_{Top})$ which can be only achieved in space
6. de/dΠ is very sensitive to the pressure difference across the melt column $(P_{gap} - P_{Top} - \rho gh)$ at small values of this pressure difference. Thus, on earth where this value is close to zero, the detachment sensitivity to perturbations in pressure is at its highest.
7. Sensitivity of the gap width ($|\partial e/\partial\theta|$) to the wetting angle decreases with increase in the wetting angle for a constant Π.
8. For the same wetting angle, systems that operate at higher Π (lower p_g) are more sensitive to the changes in the wetting angle than systems that operate at lower Π (higher p_g).

5. Quantitative stability criterion

The above analysis provides a relative framework to analyse the sensitivity of detachment gap to perturbations. It does not in of itself provide a quantitative measure of gap stability. However, a semi-quantitative measure may be obtained by analyzing these results in the context of reported experimental evidences of detached growth. In nearly all cases where the detached growth has been reported in space and not on Earth, the contact angle of the growth system has been around 120 degrees. On the other hand, our experimental evidences indicate that with a contact angle of 169 degrees detached growth is possible on Earth. Similarly for smaller contact angles we have been unable to grow detached crystals on Earth. As we do not have any information on the system pressure for the space detached growth experiments, it is not possible to map these results directly onto the data presented in this section. Nevertheless, using results of our ground-based detached experiment (GeSi in contact with PBN) our analysis would indicate that a de/dΠ of about $5\text{x}10^{-4}$ is necessary to achieve detached growth. This value of de/dΠ can be obtained for contact angles less than 169 degrees at large positive values of Π (or alternatively $P_{gap} - P_{Top} - \rho gh$). As large positive values of $P_{gap} - P_{Top} - \rho gh$ are only attainable in space (where bubble departure is not operative) detached growth for these systems can be only achieved in space.

6. Comparison With experimental Observations

The results presented above can be used to answer the following fundamental question:

Why has detached growth been reported primarily in space experiments?

As Table 1 indicates, most semiconductor/crucible systems have a contact angle not exceeding 130 degrees.

For these systems, our stability criterion of $de/d\Pi$ of about $5x10^{-4}$ is not satisfied on Earth because departure of bubbles forces the system to operate around $P_{gap} = P_{Top} + \rho gh$. Our calculations indicate that $de/d\Pi$ for contact angle of about 130 degrees at this level of gap pressure can be close to one order of magnitude higher than $5x10^{-4}$. In space, however, it is possible to operate a large values of P_{gap} with associated $de/d\Pi$ values of about $5x10^{-4}$. In space once a gas bubble is generated somehow below the growth meniscus, pressure is built up in that region and detachment is obtained. This detached gap is quite insensitive to perturbations to the system and is maintained while the crystal grows. With growth the volume of the trapped gas increases, and with no addition to the volume by mechanisms such as that proposed by Wilcox, will result in lower pressure of the gas in the detachment gap (lower P_{gap}). At some point with decreasing gap pressure P_{gap} the instability parameter increases the critical value of $de/d\Pi$ (about $5x10^{-4}$ based on these calculations). At that point in time detached growth becomes unstable. However, because there is no limit on the magnitude of gas pressure in the detachment gap at onset of growth (i.e. P_{gap} can be large) it is possible for detached growth to continue for a very long period of time; there is no theoretical factor that would inhibit achievement of detached growth for the entire crystal.

Semiconductor	Crucible	Contact Angle	Semiconductor	Crucible	Contact Angle
CdTe	p-C	116°	GaSb	p-C	128°
	p-BN	120-130°		p-BN	132°
	SiO_2	70-90°		Al_2O_3	112°
CdZnTe	p-C	126°		SiO_2	121°
InSb	p-C	124°	GaAs	SiO_2	100-115°
	p-BN	134°		p-BN	140-150°
	Al_2O_3	111°		p-C	100-120°
	SiO_2	112°			

Table 1. Contact angles for molten semiconductors

Another factor in favor of space processing is the possible magnitude of pressure perturbations. On Earth the hydrostatic head has to be accounted for in the pressure balance. Thus, the pressure difference across the melt $P_{gap} - (P_{Top} + \rho gh)$ becomes the difference between two large numbers and any change in the top or gap pressures would create a large imbalance and thus a large perturbation. In space, the pressure difference is not the difference between two large numbers and thus the possible magnitude of perturbations will be smaller.

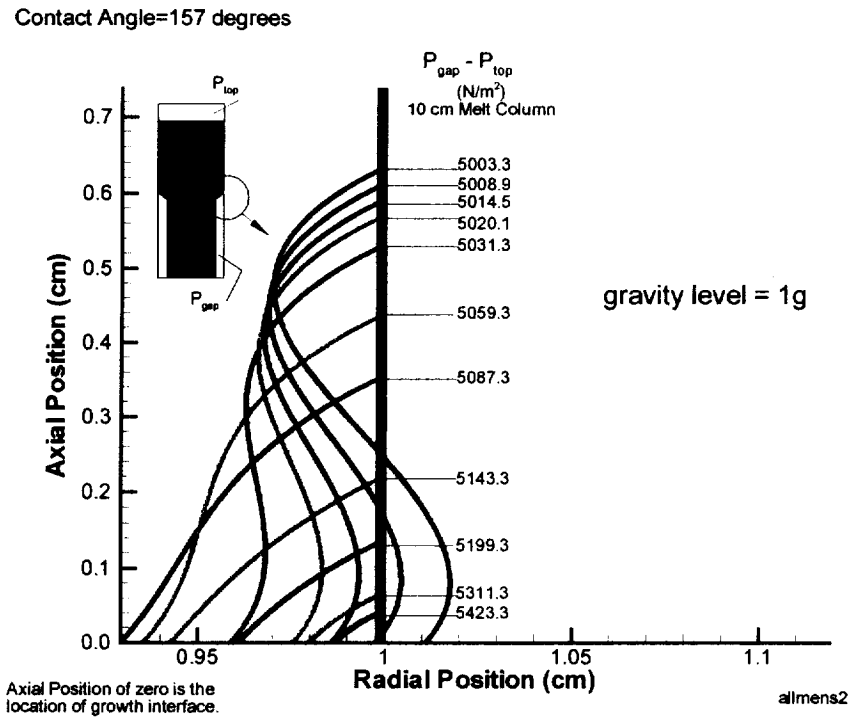

Figure 1. Menisci at different values of $P_{gap} - P_{Top}$ at 1g.

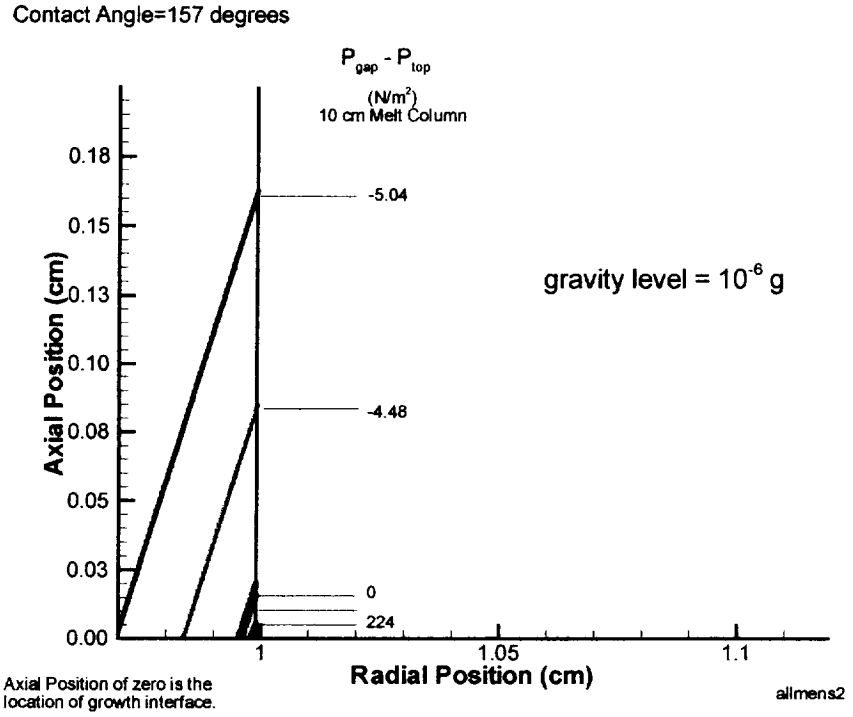

Figure 2. Menisci at different values of $P_{gap} - P_{Top}$ at micro-g.

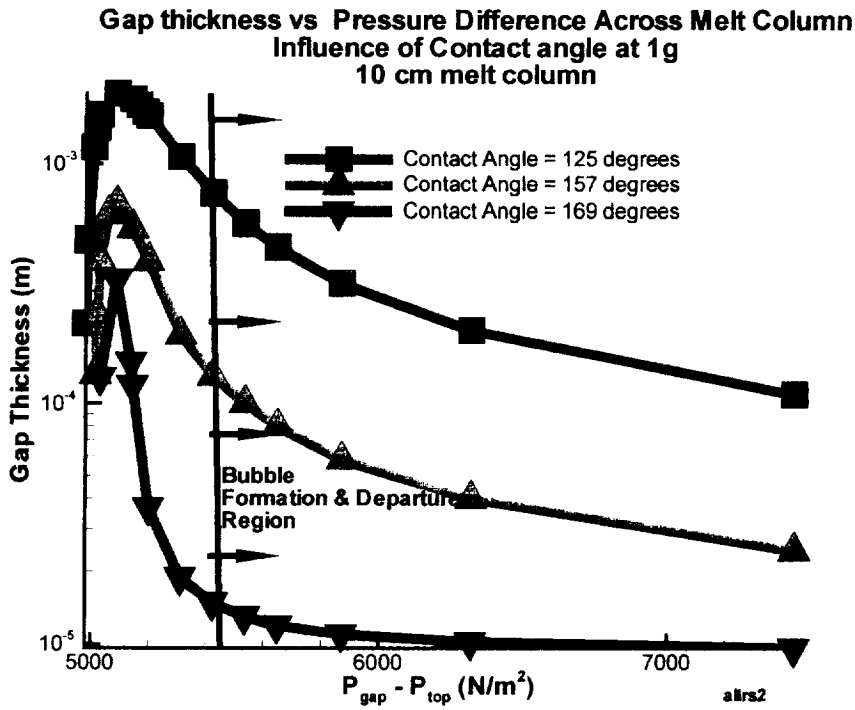

Figure 3. Variation of gap thickness with $P_{gap} - P_{Top}$ for three contact angles at 1g.

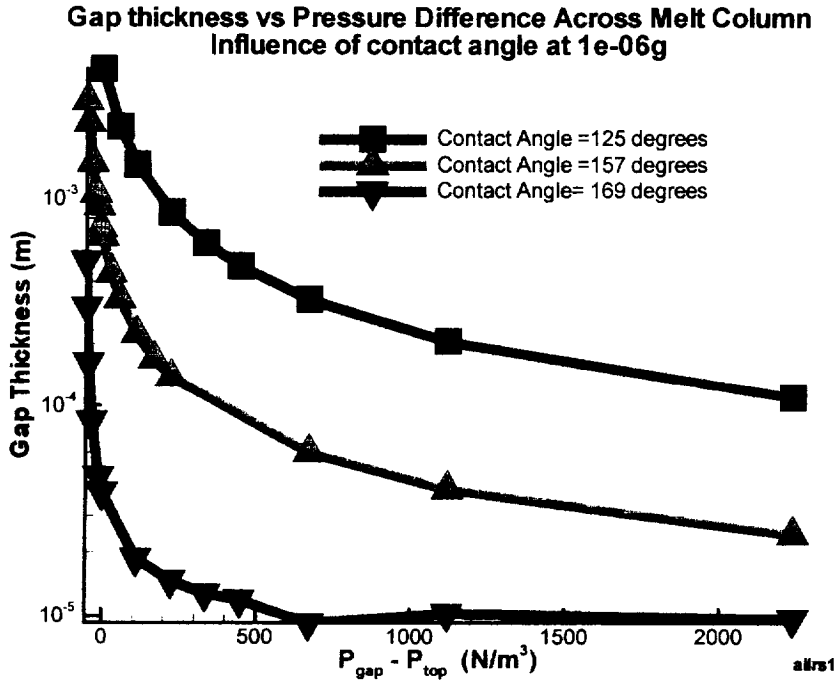

Figure 4 . Variation of gap thickness with $P_{gap} - P_{Top}$ for three contact angles at micro-g.

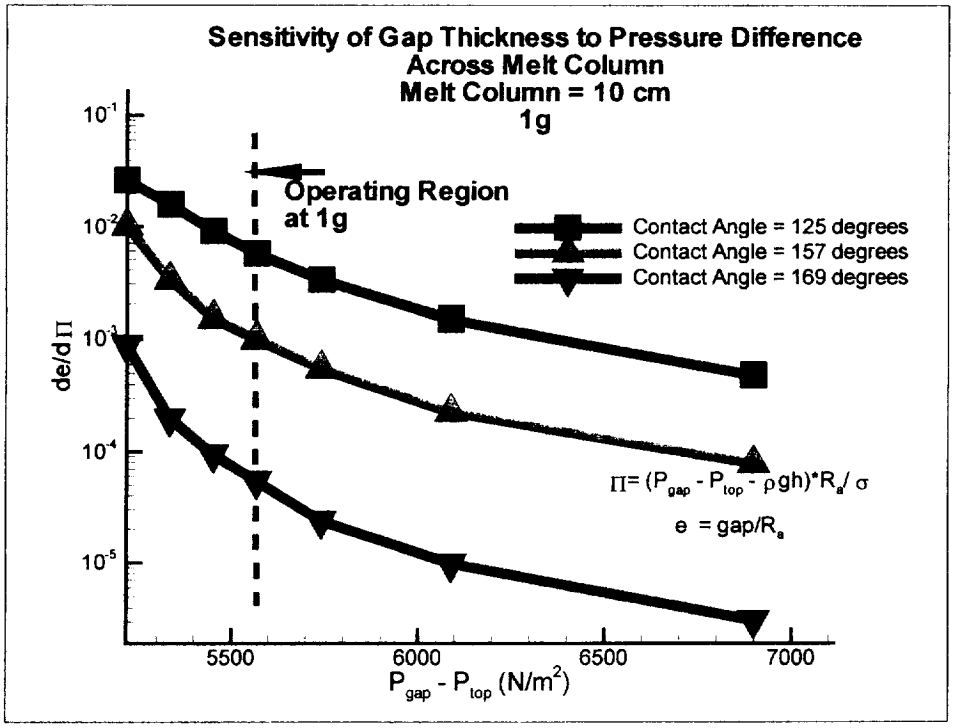

Figure 5. Sensitivity of gap thickness in terms of non-dimensional pressure (de/dΠ) versus $P_{gap} - P_{Top}$ at three contact angles at 1g.

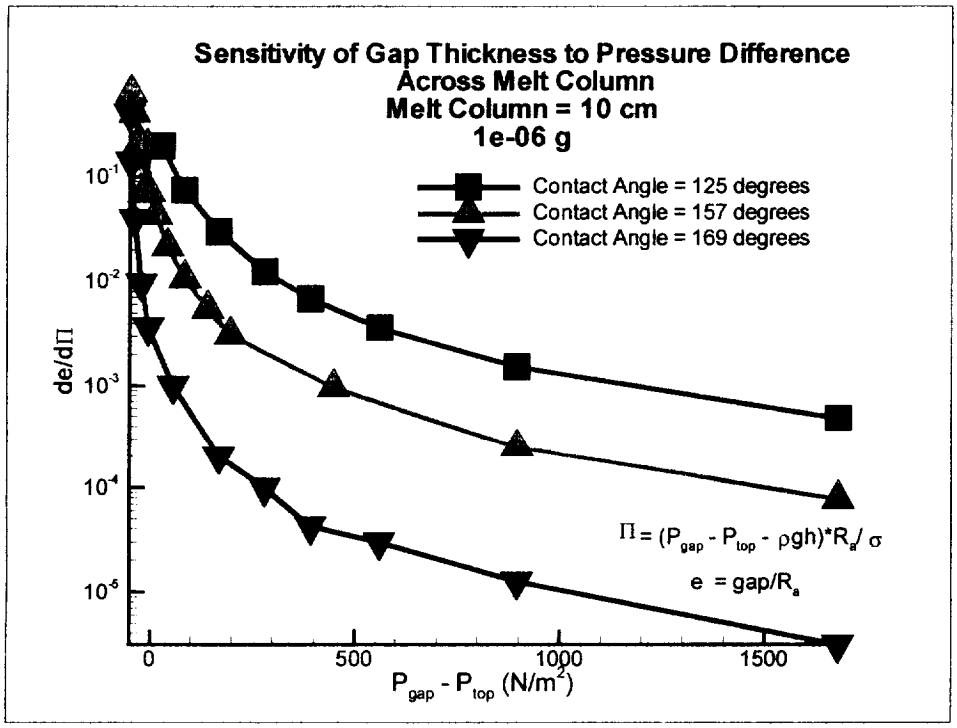

Figure 6. Sensitivity of gap thickness in terms of non-dimensional pressure (de/dΠ) versus $P_{gap} - P_{Top}$ at three contact angles at micro-g.

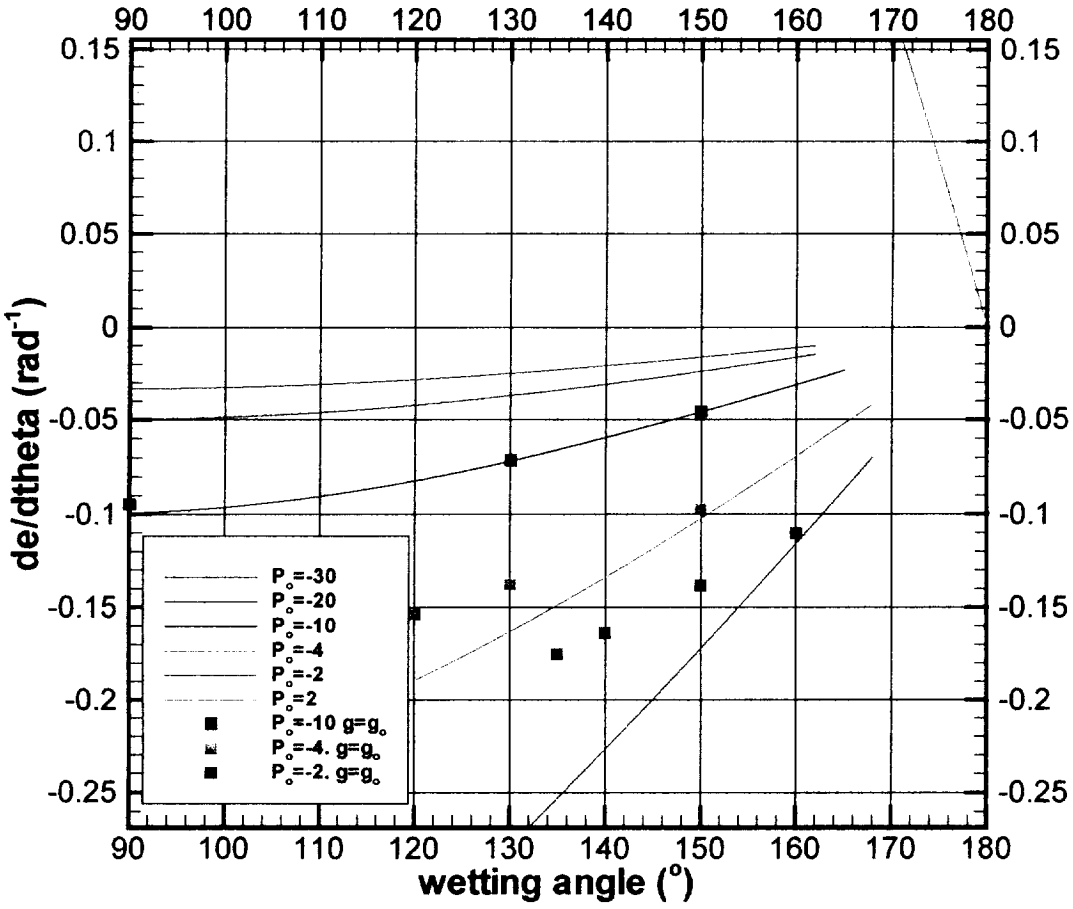

Figure 7. Sensitivity of the gap width to changes in the wetting angle as a function of the wetting angle and nondimensional pressure difference (P_o) for the zero-g and the one-g cases.

IV. Thoughts on dynamics of growth process

The growth angle γo is considered to be a material property which can be shown to be related to the surface energy balance at the melt-crystal-gas-tri-junction. It is measured as the angle made by the tangent to the growing crystal and the tangent to the meniscus, both at the tri-junction.

At steady state growth the meniscus makes the growth angle with the growing crystal. For a given set of gas pressure, hydrostatic pressure, and melt free surface pressure, the capillary force balance at the meniscus results in a meniscus shape such that it would satisfy the growth angle condition at the meniscus and the contact angle condition at the crucible wall. There is only one crystal diameter that would satisfy these conditions. Thus, for a given set of pressure parameters, the crystal diameter is determined; at steady state growth the crystal would grow at this diameter.

Now, if any one of the three pressure parameters (gas pressures, hydrostatic pressure, etc.) changes the meniscus responds fairly rapidly. The result is a meniscus shape which will not satisfy the growth angle (it may also not satisfy the contact angle; for elaboration on this point see next-to-last paragraph below). Thus the so-called melt angle (γl)will not equal the growth angle. Figure 1b shows the scenario where, for example, the pressure of the trapped gas has been increased. The system will go through a transient and re-establish a new equilibrium where the two angle conditions are satisfied. This equilibrium can be achieved only at a diameter other than the original one. Figure 1c shows the equilibrium established at a larger crystal diameter.

crystal pull rate which in effect would result in pulling or pushing on the meniscus, (b) thermal changes which would push the melting isotherm higher or lower relative to the melt free surface and thus, again, result in elongating or compressing the meniscus. In Cz-growth of Si the pull rate is used to control the diameter by changing the shape of the meniscus to compensate for the thermally-induced perturbations to the location of the growth interface (ie one end of the meniscus); In Cz-Si the growth rates are high so that changes in the pull rate influence the thermal attributes of the growth region (by changing the release of latent heat) as well as elongating/shortening the meniscus shape. Thus, the system response is much higher than it would be if changes in the pull rate were to pull/push the meniscus. In Cz-Si a plot of pull rate vs time would show very large amplitudes and relatively high frequencies.

In LEC growth of GaAs, such rapid changes in the pull rate generally results in poly growth. The approach adopted here is to put the heater controllers are an empirically-determined cooldown program such that at constant pull rate the thermal equilibrium at the growth interface (balance between heat input from melt, heat loss from the crystal

and latent heat release) is maintained with increasing crystal length, resulting in a steady meniscus shape and thus diameter during growth.

Our detached growth process and the Cz/LEC process are similar in the sense that at equilibrium crystal diameter is determined by the shape of the meniscus. There are however, several differences on how the meniscus shape is influenced. In the Cz/LEC system the melt free surface determines one end of the meniscus; the melt free surface plays the role of contact line between melt and crucible in our process. Any thermal changes in the CZ/LEC system will not have an impact on the melt free surface. Thus, by displacing the position of the growth interface (ondulating the pull rate) the meniscus shape can be modulated resulting in variations in the diameter. Changes in the thermal field, such as the growth interface shape, do not have a direct bearing on the meniscus shape: The meniscus shape determines the diameter which in turn determines heat flow at the growth interface and thus shape of solidification interface. Similarly, a change in the growth interface shape is associated with changes in the thermal field (eg reduced heat loss from crystal resulting in a more concave interface) which would result in displacing the growth interface (pushing the melting point isotherm further up into the crystal) resulting in a new meniscus shape leading to a different diameter.

In our case, we get changes in the meniscus shape primarily through changes in the pressure parameters. In case of thermal effects, let us assume that for some reason the growth rate falls behind the translation rate. Since we are translating the crucible and the charge, we do not introduce any relative displacement between the growth surface and the melt-crucible contact line. Thus, even if the heat transfer in the growth region changes resulting in a change in the growth interface shape, the only factor that will effect detachment is the changes in the pressure of the trapped gas. Within our framework, there is no other way for detachment to be influenced.

One hypothesis which we have not questioned much is the ease with which the melt-crucible contact line can slide. We implicitly assume that if we can get the necessary pressure conditions to maintain detachment, then as the crystal grows the melt-crucible line recedes at the same rate as the growth rate resulting in a steady meniscus shape. Now, if that contact line moves at a rate different from the growth rate then our detachment gap thickness would change. The fundamental question that presents itself is: what determines the speed of the melt-crucible contact line. In principle, the capillary force balance does exert a force parallel to the crucible wall at the melt-crucible contact line. It may be that as the growth interface advances and squeezes the meniscus a net axial force is generated at the melt-crucible interface that would push it upwards. Ampoule surface roughness would have an important influence here.

Our analysis is based on the quasi-steady state assumptions. That is, we calculate the equilibrium crystal diameter from the given set of process conditions. To answer the question of previous section as well as how does the meniscus actually go from on state to the other, requires dynamic simulations which would be future work (This was part of the original proposal but we cut it out because of lack of funds)

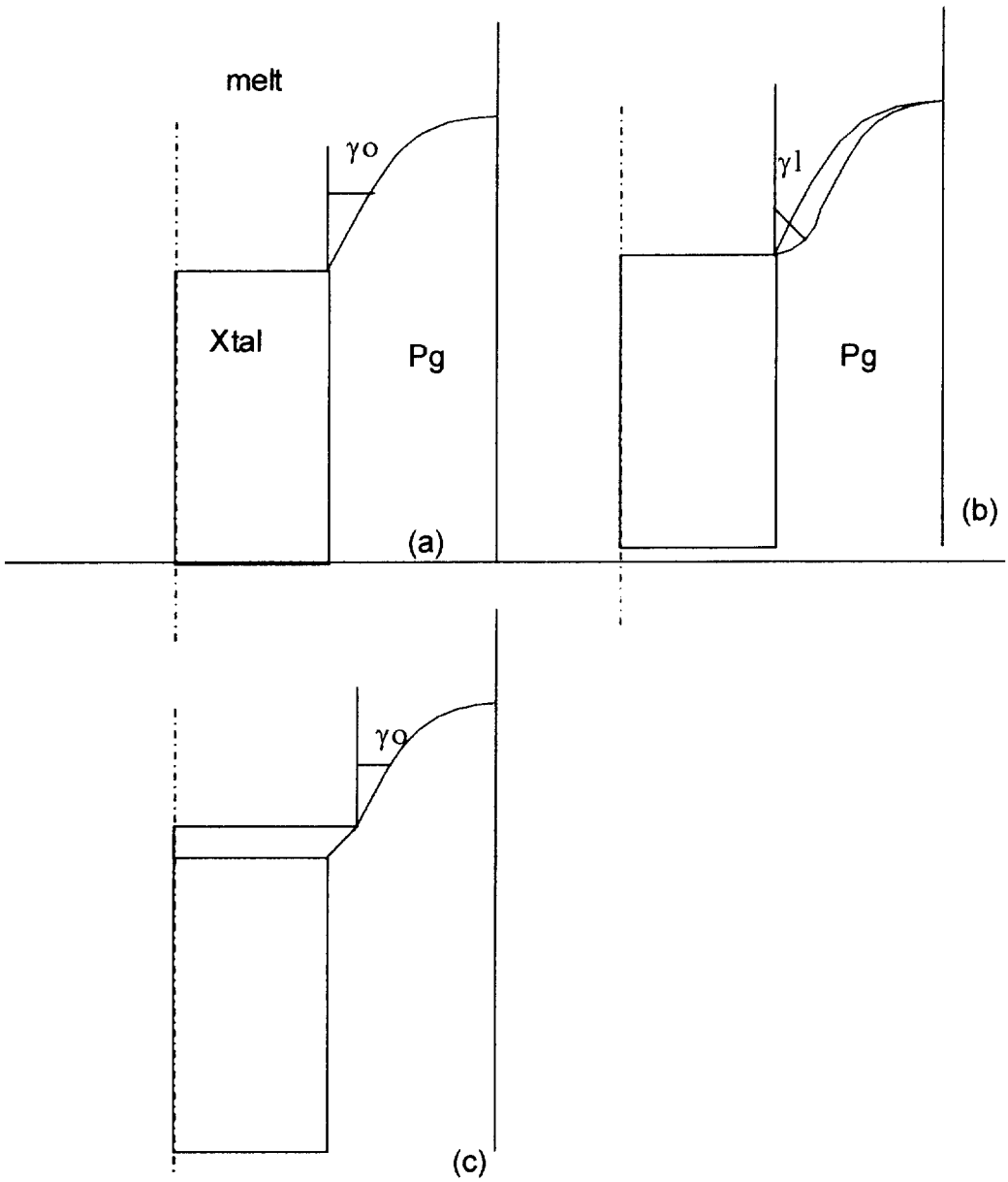

Figure 1. Response of the crystal growth process to an increase in the gas pressure p-gas.

V. Acknowledgements

The principal investigator wishes to acknowledge the collaboration and intellectual input of the staff at Cape Simulations who contributed to the development of the models, d the numerical algorithms, conducted the simulations, and compiled the results. boration of Dr. Ljubomir Vujisic, Dr. Serhat Yesilyurt, Dr. Ani Worlikar, is gratefully acknowledged.

The intellectual exchanges with NASA scientists was an essential element for the successful completion of these projects. The PI wishes to acknowledge with gratitude the support and scientific input of Dr. Frank Szofran, Dr. Donald Gillies, Dr. Martin Volz, Dr. Sharon Cobb, and Dr. Alex Lehoczky.

REPORT DOCUMENTATION PAGE

Form Approved
OMB No 0704-0188

1. AGENCY USE ONLY (Leave blank)	2. REPORT DATE	3. REPORT TYPE AND DATES COVERED

4. TITLE AND SUBTITLE

Computational Simulation of Containment Influence on Defect Generation During grwoth of GeSi

5. FUNDING NUMBERS

NAS8-98252

6. AUTHOR(S)

S. Motakef, S. Yesilyurt, L. Vujisic

7. PERFORMING ORGANIZATION NAME(S) AND ADDRESS(ES)

CAPE Simulations, Inc.
One Bridge St.
Newton, MA 02158

8. PERFORMING ORGANIZATION REPORT NUMBER

9. SPONSORING/MONITORING AGENCY NAME(S) AND ADDRESS(ES)

MSFC
MSFC, AL 35812

10. SPONSORING/MONITORING AGENCY REPORT NUMBER

11. SUPPLEMENTARY NOTES

12a. DISTRIBUTION/AVAILABILITY STATEMENT

GP23E
CN31D
LA10 PI
COTR CAI

12b. DISTRIBUTION CODE

13. ABSTRACT *(Maximum 200 words)*

This report contains results of theoretical work in conjunction with the NASA RDGS program. It is specifically focused on factors controlling the stability of detachment and the sensitivity of the detachment process to the processing and geometric parameters of the crystal growth process.

14. SUBJECT TERMS

Simulation, CRystal Growth

15. NUMBER OF PAGES

3

16. PRICE CODE

17. SECURITY CLASSIFICATION OF REPORT	18. SECURITY CLASSIFICATION OF THIS PAGE	19. SECURITY CLASSIFICATION OF ABSTRACT	20. LIMITATION OF ABSTRACT
Unclassified	Unclassified	Unclassified	None